

Charge Recombination in Undoped Cuprates

Zala Lenarčič¹ and Peter Prelovšek^{1,2}

¹*J. Stefan Institute, SI-1000 Ljubljana, Slovenia and*

²*Faculty of Mathematics and Physics, University of Ljubljana, SI-1000 Ljubljana, Slovenia*

We theoretically analyse the process of charge recombination in the planar Mott-Hubbard insulators with the aim to explain short picosecond-range lifetime of photoexcited carriers, experimentally studied via pump-probe experiments on the undoped cuprates. The recombination mechanism consists of two essential ingredients: the formation of a metastable s-type bound holon-doublon pair, i.e. the Mott exciton, and the decay of such an excitonic state via the multimagnon emission. In spite of the large gap that requires many bosons to be emitted, latter process is fast due to large exchange scale and strong charge-spin coupling in planar systems. As the starting microscopic model we consider the single-band Hubbard model, and then more realistic three-band model for cuprates, both leading to the same minimal one. The decay rate of the exciton is evaluated numerically via the Fermi golden rule, having consistency also with the direct time-evolution calculation. The decay rate reveals exponential dependence on the ratio of the Mott-Hubbard gap and the exchange coupling - the result qualitatively reproduced also within a toy exciton-boson model.

PACS numbers: 71.27.+a, 78.47.J-, 74.72.Cj

I. INTRODUCTION

Nonequilibrium properties and dynamics of strongly correlated electron systems are one of the central theoretical challenges, stimulated by the advances of ultrafast spectroscopy techniques and novel results in materials with correlated materials, as well as by the experiments on the fermionic cold atoms. One of the evident questions is the explanation of ultrafast recombination of photoinduced charges, as established in the pump-probe experiments on various materials belonging to the class of Mott-Hubbard (MH) insulators. The prominent example are undoped two-dimensional (2D) cuprates La_2CuO_4 (LCO) and Nd_2CuO_4 (NCO), representing the reference substances for the hole-doped and electron-doped high- T_c superconductors, respectively. The femtosecond pump-probe spectroscopy¹⁻³ reveals that pump pulses with photon energies above the MH gap Δ generate mobile charges, recombining in the picosecond range. This scale is many orders of magnitude shorter than in clean band insulators and semiconductors with similar gaps⁴. Photoexcited carriers in the MH insulators are in comparison to bosonic spin and phonon excitations a high-energy excitation far from equilibrium. Therefore the charge recombination process in a clean system requires an instantaneous emission of the energy $\omega > \Delta$, which demands creation of many low-energy excitations, limiting the decay rate. The evident low-energy candidates in 2D cuprates are spin excitations with the characteristic spin exchange scale J , since as the consequence of strong correlations the effective charge-spin coupling is inherently strong, and also larger than the characteristic phonon energies ω_0 . Similar questions extend to other MH materials, e.g. to the class of one-dimensional (1D) organic insulators where an ultrafast decay of photoinduced carriers was observed as well⁵⁻⁸. Closely related is the challenge of fermionic cold atoms in optical lattices where near the half-filled case the double-occupancy decay is somewhat faster^{9,10}, yet still requires many scattering processes.

Theoretical analysis of strongly correlated electron systems far from equilibrium requires novel concepts and methods due

to the failure of quasiparticle picture and Boltzmann-type approaches standard for metals and semiconductors. The relevant charge excitations in MH insulators, at least within the simplest prototype single-band Hubbard model, are empty sites - holons and doubly occupied sites - doublons. At low holon-doublon densities latter excitations bear some resemblance to the holes and electron quasiparticles in semiconductors: a) they are oppositely charged relative to the reference insulator, b) they are well mobile with an effective band dispersion within the lower and upper Hubbard band, respectively, and c) they can form a bound excitonic-like state, i.e. a holon-doublon (HD) exciton. On the other hand, unlike in a pure semiconductor a single HD pair (neglecting the coupling to phonon degrees of freedom) is not an eigenstate and has an intrinsic recombination rate Γ .

The problem of doublon decay has been addressed in the Fermi-Hubbard model in connection with ultracold fermions in optical lattices^{9,10} using the diagrammatic approach revealing an exponential dependence of the decay rate on the MH onsite repulsion U . Since in the latter case charge densities are quite high, the dominant mechanism relies on energy transfer to the kinetic energy of other fermions. The decay of double occupancy was considered also within the excited half-filled Hubbard model via the time-dependent single-site dynamical mean-field theory (DMFT)^{11,12}, for review see¹³, confirming similar $\Gamma(U)$ dependence that suggests the same recombination mechanism. One should note that besides being at rather high effective temperatures T , by construction the DMFT method does not incorporate non-local spin fluctuations. Recombination of HD pair into spin excitations at low and high temperatures has already been addressed within the n th order perturbation theory¹⁴. However, possible correlations between holon and doublon, i.e. the HD binding (an essential ingredient of our work) were neglected, since the prime interest was actually the decay of unpaired fermions in attractive Hubbard model.

Considering the case of finite photoexcited HD-pair densities $n_{HD} > 0$ the recombination processes could be qualitatively classified in analogy to semiconductors via the density

dependence of recombination rates Γ , $\Gamma \propto n_{HD}^\gamma$, into a single exponential one with $\gamma = 0$, bimolecular with $\gamma = 1$ and Auger processes with $\gamma = 2$. We elaborate in this paper the charge-recombination scenario¹⁵ relevant for undoped cuprates LCO and NCO, but also more generally for 2D MH insulators with a pronounced role of spin-fluctuation excitations. An important message from pump-probe experiments on those insulating cuprates^{2,3} is that is at least for modest pump fluences (pump intensity) the photoinduced charges (holons and doublons), measured via the probe broad-band optical pulse, decay exponentially after a very fast transient in the femtosecond range. The long-time decay rate in the picosecond range is fluence independent, i.e. independent on the initial pump intensity and corresponding initial charge density. This excludes the interpretation in terms of bimolecular and Auger processes, and leaves the option with an intermediate stage of bound HD pairs - excitons, which decay exponentially with a well defined rate. Relating back to the experiments, the initial fast transient should describe the relaxation of highly excited holons and doublons that end up in a bound HD exciton, but this is beyond our present study. The existence of a bound MH exciton with the s orbital symmetry has been shown within the planar Hubbard model that was for holons and doublons effectively reduced to 2D t - J model^{15,16}. Due to its symmetry, exciton is not directly observable by optical absorption, but is consistent with the experimental evidence of nonlinear optical susceptibility in LCO¹⁷, as well as a large Raman shift¹⁸.

In a strongly correlated system the MH exciton is not an eigenstate of the system and can decay-recombine via the emission of spin fluctuations¹⁵ with the characteristic boson scale J . Our first theoretical goal is to derive a proper perturbation term governing the decay. While in the initial study we start with the canonical transformation of the single-band Hubbard model,¹⁵ undoped cuprates are known to be charge-transfer MH insulators. In the following we show that the effective HD recombination term emerging from a more complete multi-band model of cuprates is even quantitatively similar to the one derived from the single-band model.

The HD exciton decay with the emission of a large number $n \sim \Delta/J \gg 1$ of spin fluctuations is an involved many-body problem. We calculate the recombination rate Γ within the Fermi golden rule (FGR) approach, which still requires a numerical evaluation on a small-size system. Since our results are obtained on systems with limited size this implicitly shows that long-range antiferromagnetic (AFM) order is not essential for the decay, and that energy can be transmitted to general paramagnon excitations as long as short-range AFM spin correlations are present. FGR result can be quite well verified via a direct time evolution of the HD exciton decay when the perturbation term is switched on. Quite generally Γ is well described with an exponential dependence

$$\Gamma \sim \Gamma_0 \exp(-\alpha\Delta/J), \quad (1)$$

obtained also by n th order perturbation theory arguments^{9,10,14} when considering the decay of unbound charged particles. Since α involves parameters of the model it is crucial for a fast recombination that within a MH

insulator we find $\alpha < 1$, being a consequence of the strong charge-spin coupling. While one cannot treat the effective HD model analytically, we show that there is a very helpful analogy with an exactly solvable exciton-boson (toy) model which confirms the form Eq. (1), and moreover allows direct interpretation of parameters, in particular α . The final goal of this study is the comparison with experimentally measured recombination rates in undoped cuprates NCO and LCO, and despite the fact that we propose only the minimal model for such process, obtained results are fairly close to the experimentally established ones^{2,3}.

The paper is organized as follows. In Sec. II we present the derivation of the effective model from a single-band Hubbard model via the canonical transformation. An analogous procedure is applied in Sec. III to the three-band charge-transfer model as directly relevant for undoped cuprates. Based on the existence of the bound HD exciton within the 2D effective model on a square lattice as established earlier,¹⁵ we concentrate in Sec. IV on the calculation of recombination rate Γ within the FGR approximation and on the comparison obtained with the direct time evolution. In Sec. V we present a toy exciton-boson model within which decay rate Γ can be evaluated exactly and even expressed analytically in the form analogous to Eq. (1).

II. SINGLE-BAND HUBBARD MODEL

We start with the prototype model for the studies of the MH insulator - the single-band Hubbard model,

$$H = -t \sum_{\langle ij \rangle s} (c_{js}^\dagger c_{is} + \text{H.c.}) + U \sum_i n_{i\uparrow} n_{i\downarrow}, \quad (2)$$

where sum runs over nearest-neighbor (NN) pairs of sites $\langle ij \rangle$. For the undoped cuprates the relevant lattice is 2D square lattice, which we will consider further on.

We are interested in the half-filled case, $\bar{n} = 1$, with a low density of holons $\bar{n}_h \ll 1$ and doublons $\bar{n}_d \ll 1$. When discussing the recombination we would like to work with operators causing real, not just virtual transitions. To extract them we perform the usual canonical transformation of Hubbard model¹⁹⁻²¹ that in the lowest order decouples sectors with different number of HD pairs, however still relates them perturbatively. As shown later on, the transformed Hamiltonian in addition to the standard t - J model²² contains also the terms causing recombination that were usually neglected in the studies of doped systems. Such effective model on one hand serves us to find the initial HD bound state by neglecting the recombination, and then yields its decay by taking it into account. One could perform also the transformation that completely decouples the sectors with different number of HD pairs²¹, however this would not suit our purposes.

Hence, we rederive here the effective model employing Hubbard operators X_i^{pq} , elaborated in Ref.²³. If we define the holon state as $|H\rangle = |0\rangle$ and the doublon state as

$|D\rangle = c_{i\uparrow}^\dagger c_{i\downarrow}^\dagger |0\rangle$ operators are expressed as

$$\begin{aligned} X_i^{sH} &= c_{i\bar{s}}^\dagger (1 - n_{i\bar{s}}), \quad X_i^{Ds} = -s c_{i\bar{s}}^\dagger n_{is}, \quad X_i^{DH} = s c_{i\bar{s}}^\dagger c_{i\bar{s}}, \\ X_i^{s\bar{s}} &= c_{i\bar{s}}^\dagger c_{i\bar{s}}, \quad X_i^{ss} = n_{is} (1 - n_{i\bar{s}}), \\ X_i^{HH} &= (1 - n_{i\downarrow})(1 - n_{i\uparrow}), \quad X_i^{DD} = n_{i\downarrow} n_{i\uparrow}, \end{aligned} \quad (3)$$

where $s = \pm 1$ stands for the up/down electron spins. Upper indices pq in X_i^{pq} encode the initial (q) and final (p) state after the application of the operator. In terms of the Hubbard operators the starting Hubbard model Eq. (2) can be re-expressed as

$$\begin{aligned} H &= H_U + H_t + H_{trc} = \\ &= U \sum_i X_i^{DD} - t \sum_{ij,s} (X_i^{sH} X_j^{Hs} + X_i^{D\bar{s}} X_j^{\bar{s}D}) \\ &\quad - t \sum_{ij,s} s (X_i^{sH} X_j^{\bar{s}D} + X_i^{D\bar{s}} X_j^{Hs}), \end{aligned} \quad (4)$$

where i, j are NN, and H_U, H_t, H_{trc} are the on-site-repulsion, the HD-hopping and the HD-recombination/creation terms, respectively.

A. Canonical Transformation

The canonical transformation is performed in the standard way^{19,20}

$$\tilde{H} = e^S H e^{-S} = H + [S, H] + \frac{1}{2}[S, [S, H]] + \dots \quad (5)$$

so that H_{trc} is transformed out, consequently fixing S with the condition $H_{trc} + [S, H_U] = 0$ to

$$S = \frac{t}{U} \sum_{ij,s} s (X_i^{sH} X_j^{\bar{s}D} - X_i^{D\bar{s}} X_j^{Hs}), \quad (6)$$

and the transformed Hamiltonian up to second order in t

$$\tilde{H} = H_U + H_t + [S, H_t] + \frac{1}{2}[S, H_{trc}]. \quad (7)$$

Using the X -operator commutation relations²³ we obtain several terms,

$$\tilde{H} = H_{tJ} + H_{rc} + H_c \quad (8)$$

where H_{tJ} conserves the HD number

$$\begin{aligned} H_{tJ} &= -t \sum_{ij,s} X_i^{sH} X_j^{Hs} - t \sum_{ij,s} X_i^{D\bar{s}} X_j^{\bar{s}D} + U \sum_i X_i^{DD} \\ &\quad + \frac{t^2}{U} \sum_{ij,s} (X_i^{s\bar{s}} X_j^{\bar{s}s} - X_i^{ss} X_j^{\bar{s}\bar{s}}), \end{aligned} \quad (9)$$

and H_{rc} is the essential term describing the HD recombination/creation

$$\begin{aligned} H_{rc} &= \frac{t^2}{U} \sum_{(ijk),s} s [X_k^{sH} (X_i^{ss} - X_i^{\bar{s}\bar{s}}) X_j^{\bar{s}D} + 2X_k^{\bar{s}H} X_i^{\bar{s}\bar{s}} X_j^{\bar{s}D} \\ &\quad + \text{H.c.}], \end{aligned} \quad (10)$$

where j, k are the NN sites to site i , and $j \neq k$. Further terms $H_c = H_4 + H_5 + H_6$ within the order t^2/U are

$$\begin{aligned} H_4 &= \frac{t^2}{U} \sum_{(ijk),s} s [(X_j^{sH} X_k^{\bar{s}H} - X_j^{D\bar{s}} X_k^{Ds}) X_i^{HD} \\ &\quad + X_k^{sH} X_j^{\bar{s}D} (X_i^{HH} - X_i^{DD}) + \text{H.c.}], \\ H_5 &= \frac{t^2}{U} \sum_{(ijk),s} (-X_j^{sH} X_i^{DD} X_k^{Hs} + X_j^{D\bar{s}} X_i^{HH} X_k^{\bar{s}D} \\ &\quad - X_j^{sH} X_i^{HD} X_k^{Ds} + X_j^{Hs} X_i^{DH} X_k^{sD} - X_j^{sH} X_k^{Hs} X_i^{\bar{s}\bar{s}} + \\ &\quad + X_j^{sH} X_k^{H\bar{s}} X_i^{\bar{s}s} + X_j^{D\bar{s}} X_k^{\bar{s}D} X_i^{ss} - X_j^{Ds} X_k^{\bar{s}D} X_i^{s\bar{s}}), \\ H_6 &= \frac{t^2}{U} \sum_{ij} 2(X_i^{DD} X_j^{HH} + X_i^{DH} X_j^{HD}). \end{aligned} \quad (11)$$

Within the order t^2/U the coupling between sectors with different number of HD-pairs is present in the terms H_{rc} , Eq. (10), and H_4 , Eq. (11). We note that H_4 term could be relevant for recombination only at higher HD densities, since it is active only when three charged particles are NN to each other, being negligible at $\bar{n}_d, \bar{n}_h \ll 1$. Therefore it should not play a key role in the recombination at low density of holons and doublons discussed here, and will be neglected further on. However, this term could be necessary for the description of short-time behavior in experiments where strong excitations produce an abundance of initially unbounded HD pairs. The terms H_5 and H_6 only correct the excitonic wave functions within the order t^2/U and will also be neglected in comparison to the leading H_{tJ} , Eq. (9).

B. Effective Model

The effective Hamiltonian that we consider further on contains terms Eqs. (9,10). With the introduction of holon and doublon creation and annihilation operators

$$\begin{aligned} h_{is} &= c_{i\bar{s}}^\dagger (1 - n_{i\bar{s}}) = X_i^{sH}, \\ d_{is} &= c_{i\bar{s}} n_{is} = -s X_i^{sD}, \end{aligned} \quad (12)$$

it can be written in a more compact and transparently spin-invariant way

$$\begin{aligned} H &= H_{tJ} + H_{rc} \\ H_{tJ} &= t \sum_{(ij),s} (h_{is}^\dagger h_{js} - d_{is}^\dagger d_{js} + \text{H.c.}) + U \sum_i n_{di} \\ &\quad + J \sum_{(ij)} \left(\mathbf{S}_i \cdot \mathbf{S}_j - \frac{1}{4} \delta_{1, n_i n_j} \right) \end{aligned} \quad (13)$$

$$H_{rc} = t_{rc} \sum_{(ijk),ss'} (h_{ks} d_{js'} \vec{\sigma}_{s\bar{s}'} \cdot \mathbf{S}_i + \text{H.c.}), \quad (14)$$

where $n_d = (1/2) \sum_{is} d_{is}^\dagger d_{is}$ and $\vec{\sigma} = \{\sigma^x, \sigma^y, \sigma^z\}$ is a vector of Pauli matrices. Again (ijk) signifies that j, k are the NN sites to site i , and $j \neq k$. From the derivation we obtain that the recombination term, Eq. (14), has the coupling parameter $t_{rc} = 2t^2/U = J/2$.

III. CHARGE-TRANSFER HUBBARD MODEL

It is well known that on a microscopic level undoped and doped cuprates cannot be fully described within the single-band Hubbard model, since they are undoped or doped Mott insulators of the charge-transfer type, where more orbitals have to be included in the starting microscopic model. Therefore it is sensible to verify whether the recombination couplings obtained from the canonical transformation of the single-band Hubbard model are qualitatively correct approximation for the description of 2D cuprates. We take the accepted multi-band tight-binding model for electrons on the 2D CuO₂ layers, including $3d_{x^2-y^2}$ orbitals on Cu atoms and $2p_x/2p_y$ on O atoms.²⁴⁻²⁸ In contrast to numerous theoretical studies and models of hole doped systems, both type of charge carriers, positive and negative, have to be treated on the same level of approximation²⁹⁻³¹ in the present case of excited MH insulator with holons and doublons.

A. Multi-band Model

In the following, states are as usual (but in contrast to the previous section) defined relative to the filled 3d orbitals on copper and 2p orbitals on oxygen²⁶. Including the NN Cu-O and O-O hopping, and the Coulomb repulsion on/between Cu and O orbitals, the three-band p - d model is written as

$$H = \sum_{is} \epsilon_i n_{is} + \sum_{\langle ij \rangle s} t_{ij} (c_{is}^\dagger c_{js} + \text{H.c.}) + \sum_i U_i n_{i\uparrow} n_{i\downarrow} + \sum_{\langle ij \rangle} V_{ij} n_i n_j. \quad (15)$$

Here c_i (with corresponding n_i) stands for the annihilation of holes on different orbitals, therefore equals either $c_i \equiv \bar{d}_i$ for d orbitals with energy ϵ_d on copper at site i or $c_i \equiv p_{xi}$ (p_{yi}) for p orbitals with energy ϵ_p on oxygen with positive displacement x (y) relative to the NN copper at site i . We use notation \bar{d} to avoid further confusion with doublon operators. Hopping parameters equal $|t_{ij}| = t_{pd}, t_{pp}$ for hopping between NN Cu-O and O-O orbitals, respectively, with sign dependent on the phases of facing orbitals. Parameters $U_i = U_d, U_p$ take into account the on-site Coulomb repulsion on Cu and O orbitals, respectively, while $V_{ij} = V_{pd}$ accounts for the repulsion between neighboring Cu-O orbitals. Introduced parameters have been extensively discussed in the literature. For numerical estimates further on we use the concrete values $\epsilon_p - \epsilon_d = 2.7, t_{pd} = 1, t_{pp} = 0.5, U_d = 7, U_p = 3, V_{pd} = 1$, all in units of $t_{pd} \approx 1.3eV$, as used by others^{28,29}.

In the analysis we retain only a symmetrized oxygen orbital $(1/2)(|p_x\rangle - |p_y\rangle - |p_{-x}\rangle + |p_{-y}\rangle)$, the one that hybridizes with the $d_{x^2-y^2}$ orbitals, leading to a two-band model²⁵⁻²⁷. Furthermore, we introduce their combinations - the orthonormal Wannier orbitals²⁵, in framework of which the Hamiltonian can be separated into two parts: the local Hamiltonian H_0 describing the noninteracting cells, and the inter-cell coupling term H_{cc} . Each cell contains a Cu orbital and a Wannier

O orbital. Local part of the Hamiltonian has the form of a sum $H_0 = \sum_i \mathcal{H}_{0i}$ of local intra-cell terms

$$\mathcal{H}_{0i} = \Delta_0 \sum_s n_{is}^p - \bar{t}_{pd} \sum_\sigma (\bar{d}_{is}^\dagger p_{is} + \text{H.c.}) + U_d n_{i\uparrow}^\bar{d} n_{i\downarrow}^\bar{d} + \bar{U}_p n_{i\uparrow}^p n_{i\downarrow}^p + \bar{V}_{pd} \sum_{ss'} n_{is}^\bar{d} n_{is'}^p, \quad (16)$$

where p_i^\dagger creates hole in the O Wannier orbital. Within the Wannier-orbital transformation parameters equal $\Delta_0 = \epsilon_p - \epsilon_d - 1.45 t_{pp}, \bar{t}_{pd} = 1.92 t_{pd}, \bar{U}_p = 0.21 U_p, \bar{V}_{pd} = 0.92 V_{pd}$, as taken from Ref.²⁹. In the inter-cell part H_{cc} we retain only the dominant Cu-O and the O-O hopping,

$$H_{cc} = 2t_{pd}\mu_{10} \sum_{ijs} (\bar{d}_{is}^\dagger p_{js} + p_{is}^\dagger \bar{d}_{js}) + 2t_{pp}\nu_{10} \sum_{ijs} p_{is}^\dagger p_{js}, \quad (17)$$

with coefficients $\mu_{10} = 0.14, \nu_{10} = 0.27$ for NN i and j sites, as taken from^{29,30}.

B. Local Charge and Spin States

To discuss the recombination between holons and doublons we first have to identify states that represent them. Using the hole picture, doublon is represented by the filled Cu orbital, hence being the vacuum state $|D\rangle = |0\rangle$. On the other hand, holon is the generalized Zhang-Rice singlet^{25,29} $|H\rangle = H^\dagger|0\rangle$, obtained as the g.s. of local Hamiltonian \mathcal{H}_0 in the singlet spin sector spanned by the states

$$\frac{1}{\sqrt{2}}(\bar{d}_\uparrow^\dagger p_\downarrow^\dagger - \bar{d}_\downarrow^\dagger p_\uparrow^\dagger)|0\rangle, \bar{d}_\uparrow^\dagger \bar{d}_\downarrow^\dagger|0\rangle, p_\uparrow^\dagger p_\downarrow^\dagger|0\rangle, \quad (18)$$

and has energy E_H . The single-hole state $|g_s\rangle$ (having correspondence to the spin background states in the single-band model) is calculated as the g.s. of \mathcal{H}_0 within the doublet sector spanned by

$$\bar{d}_s^\dagger|0\rangle, p_s^\dagger|0\rangle \quad (19)$$

and has energy E_g . Besides the latter, we consider also the triplet states

$$|T_0\rangle = \frac{1}{\sqrt{2}}(\bar{d}_\uparrow^\dagger p_\downarrow^\dagger + \bar{d}_\downarrow^\dagger p_\uparrow^\dagger)|0\rangle, \\ |T_{-1}\rangle = \bar{d}_\downarrow^\dagger p_\downarrow^\dagger|0\rangle, |T_1\rangle = \bar{d}_\uparrow^\dagger p_\uparrow^\dagger|0\rangle \quad (20)$$

with energy E_T . Other states, i.e. excited states within each sector, which can also be obtained with the diagonalization of H_0 , will be neglected in our further analysis. Having higher energies they might be needed for the proper description of the early dynamics after the pump excitation, when highly excited states might be created. However, after the initial relaxation, we assume that system can be represented by the lowest lying states (which still represent also the excitations across the charge-transfer gap).

Although states $|H\rangle, |D\rangle, |g_s\rangle$ are a combinations of Wannier orbitals each of them is attributed to a single cell. Moreover, the hybridization between copper and oxygen orbitals,

intrinsically present in them (as a consequence of basis vectors or diagonalization procedure), turns out essential when addressing the inter-cell hopping matrix elements of H_{cc} , Eq. (17), as discussed in App. B. Still, they obviously bridge the single- and multi-band consideration by having analogues in the single-band picture.

C. Reduced Hamiltonian

We can now proceed by writing the effective Hamiltonian in analogy with the single-band one by using the relevant states introduced in the previous subsection. It is convenient to write the Hamiltonian with X operators, analogously to those in the single-band model, Eq. (3),

$$\begin{aligned}\bar{X}_i^{sD} &= g_{is}^\dagger (1 - n_i^d)(1 - n_i^p), \\ \bar{X}_i^{sH} &= g_{is}^\dagger H_i, \quad \bar{X}_i^{sT_{s'}} = g_{is}^\dagger T_{is'}, \\ \bar{X}_i^{ss} &= g_{is}^\dagger g_{is}, \quad \bar{X}_i^{s\bar{s}} = g_{is}^\dagger g_{i\bar{s}}, \\ g_s^\dagger &= \cos \theta (1 - n_s^d)(1 - n_s^p) \bar{d}_s^\dagger + \sin \theta (1 - n_s^p)(1 - n_s^d) p_s^\dagger\end{aligned}\quad (21)$$

where $g_{is}^\dagger, H_i^\dagger, T_{is}^\dagger$ create the doublet g.s., holon (generalized Zhang-Rice singlet) and the triplet state, respectively. It still holds that $\bar{X}_i^{AB} = (\bar{X}_i^{BA})^\dagger$. Again $s = \pm 1$ associated with g_{is} stands for hole spin, whereas in T_{is} it can have values $s = \pm 1, 0$ according to definitions in Eqs. (20). To insure X_i^{As} is nonzero only when applied to doublet g.s., its creation operator is written out explicitly, using parametrization elaborated in App. A. In terms of such X operators we can present the Hamiltonian as the sum $H = H_t + H_{trc} + H_{dg}$, representing the effective HD hopping (containing possible creation of triplet states), their recombination and the diagonal part, respectively,

$$\begin{aligned}H_t &= \sum_{ij,s=\pm 1} (t^h \bar{X}_i^{Hs} \bar{X}_j^{sH} + t^d \bar{X}_i^{sD} \bar{X}_j^{Ds}) \\ &+ \sum_{ij,s=\pm 1} (-s t^{T_0} \bar{X}_i^{sH} \bar{X}_j^{T_0s} + s t^{T_1} \bar{X}_i^{s\bar{H}} \bar{X}_j^{T_1s} + \text{H.c.}) \\ H_{trc} &= \sum_{ij,s=\pm 1} (-s t^r \bar{X}_i^{sH} \bar{X}_j^{sD} + t^{r_0} \bar{X}_i^{sT_0} \bar{X}_j^{sD} \\ &+ t^{r_1} \bar{X}_i^{sT_s} \bar{X}_j^{sD} + \text{H.c.}) \\ H_{dg} &= \sum_i (\epsilon_H \bar{X}_i^{HH} + \epsilon_D \bar{X}_i^{DD} + \epsilon_T \sum_{s=\pm 1, 0} \bar{X}_i^{T_s T_s}),\end{aligned}\quad (22)$$

$$(23)$$

$$(24)$$

where i, j are NN. Values $\epsilon_H = E_H - E_g, \epsilon_D = -E_g, \epsilon_T = E_T - E_g$ are the single-cell energies of holon, doublon and triplet relative to the doublet g.s., respectively. Dependence of the introduced couplings $t^c, c = h, d, T_0, T_1, r, r_0, r_1$ and energies $\epsilon_H, \epsilon_D, \epsilon_T$ on the parameters of the original Hamiltonian Eqs. (16,17) is presented in the App. B.

D. Effective Hamiltonian

Similarly to the treatment of the single-band Hubbard model within the $U \gg t$ limit in Sec. II we transform out the recombination/creation term H_{trc} with a canonical transformation $e^S H e^{-S}$. Operator S is determined by the condition $[S, H_{dg}] + H_{trc} = 0$. After the transformation, HD recombination/creation term H_{rc} again acts between the next-NN cells, however, now one has to distinguish between channels leading to different configurations of spins in the doublets of final state, since their amplitudes r^i are different

$$\begin{aligned}H_{rc} &= - \sum_{(ijk),s} s [\bar{X}_k^{sH} (r^h \bar{X}_i^{ss} - r^d \bar{X}_i^{s\bar{s}}) \bar{X}_j^{sD} \\ &+ r^{hd} \bar{X}_k^{s\bar{H}} \bar{X}_i^{s\bar{s}} \bar{X}_j^{sD} + \text{H.c.}], \\ r^h &= \left(\frac{t^h t^r}{\epsilon_H + \epsilon_D} + \frac{t^{T_0} t^{r_0}}{\epsilon_T + \epsilon_D} \right), \\ r^d &= \left(\frac{t^d t^r}{\epsilon_H + \epsilon_D} - \frac{t^{T_1} t^{r_1}}{\epsilon_T + \epsilon_D} \right), \\ r^{hd} &= \left(\frac{(t^d + t^h) t^r}{\epsilon_H + \epsilon_D} - \frac{t^{T_0} t^{r_0}}{\epsilon_T + \epsilon_D} \right).\end{aligned}\quad (25)$$

$$(26)$$

Not only different amplitudes of holon and doublon hopping parameters, but also new processes of recombination via intermediate triplet states alter the result. To obtain the latter, hopping terms involving triplet states were included in H_t and H_{trc} in the first place. Although they exhibit richer physics of multi-band model, one should be aware that recombination via triplet state causes only smaller corrections in the coupling strengths, since $\epsilon_H \ll \epsilon_T$. However, pure form of Eq. (25) is very similar to its single-band analogue Eq. (10) with an additional overall minus that is a consequence of transition from electron to hole picture.

If we calculate all three relevant recombination couplings $2r^d, r^{hd}, 2r^h$ at realistic parameters we confirm that they are not far away from $t_{rc} = J/2$, the value obtained from the single-band model. Their dependence on Δ_0 is plotted in Fig. 1. Rescalations are made for clearer comparison with $J/2$. Using the same procedure via intra-cell diagonalization, exchange coupling plotted is expressed as²⁹

$$J = 4 \left(\frac{(t^r)^2}{\epsilon_H + \epsilon_D} - \frac{(t^{r_0})^2}{\epsilon_T + \epsilon_D} \right).\quad (27)$$

To exhibit the spin invariance of H_{rc} we define (as in the single-band model) $\tilde{d}_{is} = -s \bar{X}_i^{sD}, \tilde{h}_{is} = \bar{X}_i^{sH}$ in term of which H_{rc} obtains a form similar to Eq. (14),

$$H_{rc} = - \sum_{(ijk)ss'} \left[\tilde{h}_{is} \tilde{d}_{ks'} (r^{hd} \vec{\sigma}_{s\bar{s}'} \cdot \mathbf{S}_j + \bar{r}^{hd} \mathbb{1}_{s\bar{s}'}) + \text{H.c.} \right],\quad (28)$$

where we used $\bar{r}^{hd} = (r^h - r^d)/2$ and $t^{T_1} t^{r_1} = 2t^{T_0} t^{r_0}$, see App. B.

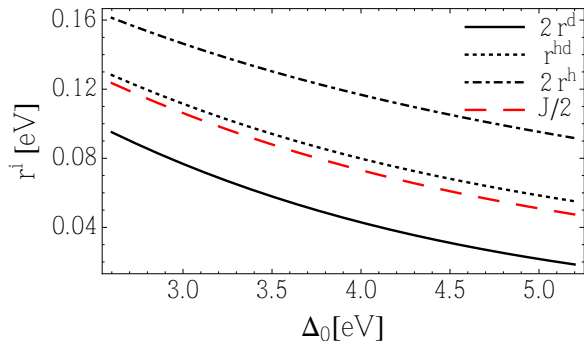


Figure 1. (Color online) Comparison of coupling parameters $r^i = 2r^d, r^{hd}, 2r^h$ for different recombination channels with the (rescaled) exchange coupling $J/2$ as a function of charge-transfer gap Δ_0 . For other parameters standard values are used.

IV. EXCITON RECOMBINATION RATE

In previous Secs. II, III it was shown that both the single-band Hubbard model as well as the three-band model for cuprates reduce at low HD density to the same effective model with the only difference being the strengths of the recombination/creation terms in H_{rc} .

A. Holon-doublon Exciton

In order to explain the experimentally observed independence of decay rate Γ on the pump fluence, i.e. also the exponential decay of HD density, we first have to determine the existence of the bound HD pair. This is based on argumentation that if pairs were not bound, recombination process would depend on the probability to encounter the oppositely charged particle, evidently leading to a non-exponential decay (unless thermal charge density is high). Present problem of HD binding has analogies with binding of holes in doped cuprates, also studied withing the t - J model^{22,32}. Although the origin of binding is in both cases the same, indistinguishable two holes $N_h = 2$ form a d -type bound state, whereas the distinguishable doublon and holon form a s -type (A_1 symmetry) bound pair, which is indeed found numerically^{15,16}. Since latter state has even symmetry it is not accesible by optical transition from the insulator AFM state. On the other hand, the optically active p -type state with binding energy $\epsilon_b \gtrsim 0$ within our calculation does not seem to be a bound one.

Knowing that at low charge density coupling between sectors with different number of HD pairs is weak, we first neglect the recombination/creation term H_{rc} that causes transitions between sectors, and extract the initial HD state $|\psi_0^{hd}\rangle$ from the spectrum of eigenstates of $H_{t,J}$, Eq. (13), as the g.s. in the sector with one HD pair. Calculating it in the single HD pair sector for system of limited size we neglect possible interaction between different pairs, justified for the cases of low charge density.

Binding properties of HD state $|\psi_0^{hd}\rangle$ were obtained via ex-

act diagonalization of $H_{t,J}$ using the Lanczos technique on the square lattices with $N \leq 26$ sites and periodic boundary conditions. Here we shall skip the detailed analysis and results presented in Ref.¹⁵. In short, we calculated the HD binding energy $\epsilon_b = E_0^{hd} - E_0^h - E_0^d + E_0^0$ where $E_0^{hd}, E_0^h, E_0^d, E_0^0$ correspond to the HD pair, single hole, single doublon and the undoped AFM g.s., respectively. In the regime of interest for cuprates ($J/t = 0.3 - 0.4$) the lowest (s -type) state shows appreciable binding $\epsilon_b/t \sim -0.4$, quite robust towards the finite size effects¹⁵. It should be pointed out that the inclusion of longer-range Coulomb repulsion would even enhance $|\epsilon_b|$ but is not expected to be the driving or dominant effect (results presented in Ref.¹⁵) in the 2D square lattice. As an additional proof of HD binding we calculate also the exciton density correlations $D_j = \langle \psi_0^{hd} | n_{hj} n_{d0} | \psi_0^{hd} \rangle$ (for the purpose of presentation the position of doublon is chosen as the origin). D_j obtained on $N = 26$ for $J = 0.4$ are presented in Fig. 2, showing consistence with the binding since HD pair is with the largest probability on a distance $d_0 = \sqrt{2}$, as is also the case for the d -wave hole binding within the 2D t - J model^{22,32}.

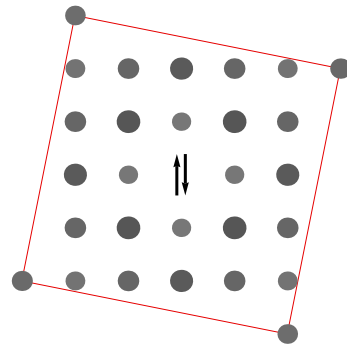


Figure 2. (Color online) Charge density correlation D_j .

B. Recombination Rate via Fermi Golden Rule

The HD exciton $|\psi_0^{hd}\rangle$ is not an eigenstate of the effective model when perturbation H_{rc} , Eq. (14), is included. A standard approach to evaluate the decay rate into a continuum of states is the Fermi golden rule,

$$\Gamma = 2\pi \sum_m |\langle \psi_m^0 | H_{rc} | \psi_0^{hd} \rangle|^2 \delta(E_m^0 - E_0^{hd}), \quad (29)$$

where the matrix elements are highly nontrivial since they represent the overlap of modified exciton wave function $H_{rc}|\psi_0^{hd}\rangle$ on highly spin-excited (multi-magnon) states $|\psi_m^0\rangle$ with energy E_m^0 within the undoped AFM spin system. Our application of the FGR approximation has many analogies, recently employed in the analysis of the decay of excitons via multi-phonon emission in nanotubes^{33,34}. For the numerical consideration it is crucial that Eq. (29) can be represented as a resolvent $\Gamma = -2 \text{Im}C(\omega = \Delta)$, where $\Delta = E_0^{hd} - E_0^0$ is

the excitation gap, and

$$C(\omega) = \langle \psi_0^{hd} | H_{rc} \frac{1}{\omega^+ + E_0^0 - H_J} H_{rc} | \psi_0^{hd} \rangle, \quad (30)$$

with $\omega^+ = \omega + i\delta$. In the evaluation only the exchange part H_J of the H_{tJ} , Eq. (13), is relevant.

Within Lanczos procedure Eq. (30) can be evaluated^{22,35} on 2D square lattice with up to $N = 26$ sites¹⁵. In Fig. 3 the dependence $\Gamma(\Delta)$ for $J = 0.3, 0.4, 0.6$ is presented. Here the energy of HD pair Δ that has to be transmitted to the spin excitations, $\Delta = E_m^0 - E_0^0$, is taken as a parameter independent of J . As suggested from Fig. 3 decay rate Γ shows approximately exponential dependence on Δ/J , Eq. (1), with effective α in the range $0.3 < \alpha < 0.7$ (for chosen $0.3 \leq J \leq 0.6$). This signals that there is some additional subtle J dependence, besides the exponential dependence on the number of spin excitations $n \sim \Delta/J$ created.

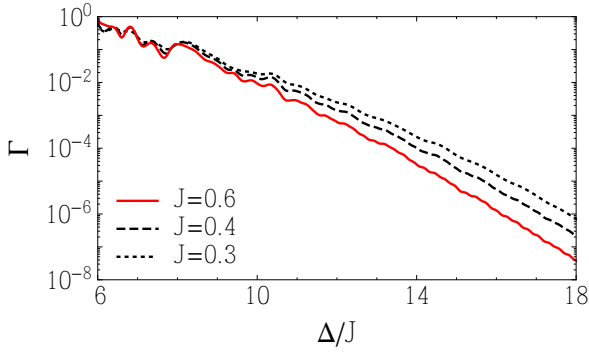


Figure 3. (Color online) Exciton recombination rate Γ vs. Δ/J for different $J = 0.3, 0.4, 0.6$ as calculated for $N = 26$ sites.

As discussed already in Ref.¹⁵ essential ingredient for the substantial decay is dressing of HD pair with spin excitations, revealed by deviations in bond energy of the exciton state relative to the AFM g.s.¹⁵. In the process of recombination this local spin perturbation can be even enhanced, and finally has to disperse into the whole system. An attempt to relate both aspects is to motivate the dependence of decay rate on Δ and J via the construction of sufficient spin dressing of cca. n spin flips as a n -th order perturbation process¹⁵, as suggested by previous similar considerations^{9,10,14}. According to these arguments, following from the appropriate matrix element, decay rate should have the form

$$\Gamma \propto \exp \left[-\alpha_0 \frac{\Delta}{J} \ln \frac{\Delta}{et} \right]. \quad (31)$$

with $\alpha_0 = 2$. However, when fitting Eq. (31) to the numerical data, $\alpha_0 \approx 0.8$ with modest J dependence is obtained¹⁵. In Ref.¹⁴ the additional structure of constant α_0 was treated with self-avoiding path reasoning, though not for the bound HD pair. Our more elaborate, however not necessarily unrelated consideration of charge-spin coupling using exciton-boson model will be given in the next section.

C. Recombination Rate via Direct Time Evolution

In order to validate the approximation using the FGR, Eq. (29), we perform also direct time evolution of the same initial excitonic state $|\psi_0^{hd}\rangle$ under the whole Hamiltonian $H = H_{tJ} + H_{rc}$, however, we restrict the Hilbert space only to the sectors with zero and one HD pair. In Fig. 4 we present the time evolution of the doublon (also the HD pair) occupation number,

$$n_d(\tau) = \frac{1}{2} \langle \psi(\tau) | \sum_{is} d_{is}^\dagger d_{is} | \psi(\tau) \rangle. \quad (32)$$

The evolution of $|\psi(\tau)\rangle$ is obtained by solving the time-dependent Schrödinger equation using the Lanczos method^{35,36}. In Fig. 4 we present and compare results for $J = 0.4$ and different effective gaps $\Delta = 4.8, 5.2, 6.0$, as calculated for the system with $N = 26$ sites. Effective gap is defined using $|\psi_{gs}\rangle$ (g.s. of H within our restricted Hilbert space) as

$$\Delta = \langle \psi_0^{hd} | H | \psi_0^{hd} \rangle - \langle \psi_{gs} | H | \psi_{gs} \rangle, \quad (33)$$

since it turns out to be a function of the coupling strength t_{rc} due to adiabatic change of the eigenspectra of H caused by H_{rc} . By adiabatic we mean that even though the whole energy of each eigenstate is shifted, the fraction of spin excitations within it is preserved, and it is the amount of spin excitations that should label the final states when discussing the recombination. Rapid oscillations seen in Fig. 4 emerge due to fast switching of H_{rc} and finite-size effects, however, they get evidently reduced with bigger N . For clarity averaging over $\delta\tau = 3$ is used.

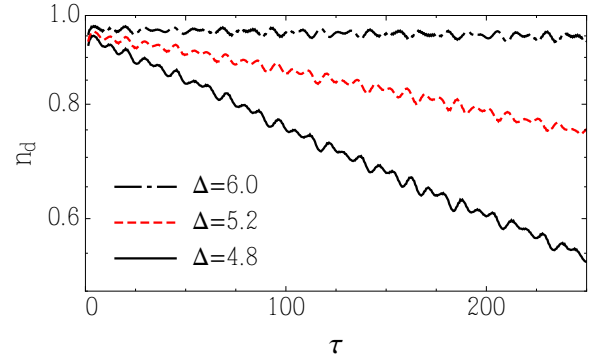


Figure 4. (Color online) Doublon (and also HD pair) occupation number n_d (in logarithmic scale) as a function of time τ , calculated for different gaps $\Delta = 4.8, 5.2, 6.0$ and parameters $J = 0.4$ for system of size $N = 26$.

From Fig. 4 we can confirm that after an initial transient an exponential decay is established. When simulating recombination on a finite system one should be aware that the finite-size level distance $\delta\omega$ limits the long-time evolution to $\tau \approx 2\pi/\delta\omega$, and is for system with $N = 26$ sites of order $\delta\omega \approx 10^{-1}$. Using the fit $\log n_d(\tau) = -\Gamma\tau + \log n_{d0}$, one can compare the result obtained for Γ with the one calculated

with FGR. Fig. 5 shows this comparison for $J = 0.4$ and system sizes $N = 20, 26$. Lines correspond to the result from FGR, while dots are obtained from the fits to $\log n_d(\tau)$ in the span of interesting Δ . We obtain a quite good agreement between the two methods, as shown in Fig. 5. Both methods confirm the exponential dependence Eq. (1). Somewhat smaller Γ obtained with time evolution on $N = 20$ lattice could be attributed to the decay into the discrete multi-magnon spectra, which is sparser at smaller lattices.

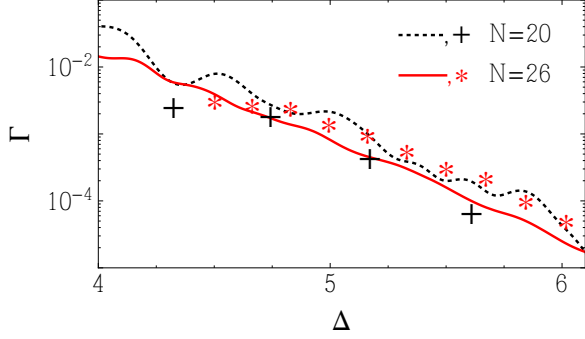


Figure 5. (Color online) Comparison of the exciton recombination rate Γ vs gap Δ as calculated using the FGR (lines) and time evolution (dots) for $J = 0.4$ and systems of size $N = 20, 26$.

V. COUPLED EXCITON - BOSON MODEL

Our numerical results clearly reveal approximate exponential dependence of decay rate Γ , Eqs. (1), on the number of bosonic excitations $n \sim \Delta/J$ created in the recombination process. As mentioned in the previous section such dependence has been reproduced qualitatively also via the n -th order perturbation arguments^{9,10,14,15}, yet the constant $\alpha_0 \approx 0.8$ obtained from fitting Eq. (31) to numerical results cannot be given a clear origin. It would be desirable to have a solvable model, which could qualitatively or even quantitatively simulate the observed physics. Relying on the interpretation developed in the previous section; suggesting that in the process of recombination spin excitations dressing the HD pair are dispersed into the whole system, it seems plausible to formulate the problem more generally - as a decay of an excitonic state $|e\rangle = e^\dagger|0\rangle$ due to coupling to bosonic degrees of freedom. The main physics of such formulation can be captured with an exciton-boson toy model, used on a similar problem to interpret the charge recombination in carbon nanotubes via the multi-phonon emission^{33,34}, here generalized to dispersive bosons,

$$\begin{aligned} H &= H_e + H_{eb} + H_b + H_{rc} \\ &= E_e e^\dagger e + e^\dagger e \sum_q \lambda_q (a_q^\dagger + a_{-q}) + \sum_q \omega_q a_q^\dagger a_q + \\ &\quad + g_{rc} (e + e^\dagger). \end{aligned} \quad (34)$$

a_q^\dagger is creation operator for bosons with momentum q and energy ω_q . The exciton-boson coupling is mediated by the term H_{eb} , while H_{rc} represents the simplest form of the exciton recombination/creation. It is evident that such model only indirectly simulates the full physics of exciton coupled to spin fluctuations, Eqs. (13,14).

The toy model Eq. (34) basically describes the two-level system coupled to bosons, and was used when discussing related question of radiationless transitions in large molecules³⁷, quantum dissipation³⁸, and in numerous other problems. It is well analyzed and solvable in several limits, in particular if H_{rc} is treated as a perturbation.

Drawing analogies with procedure in the previous section, we would like to obtain the excitonic wave function dressed with bosons and get rid of the strong coupling between exciton and bosons on the level of unperturbative part of the Hamiltonian. Therefore we do the standard Lang-Firsov transformation $\tilde{H} = e^{-S} H e^S$, which eliminates H_{eb} with

$$S = -e^\dagger e \sum_q \alpha_q (a_q^\dagger - a_{-q}), \quad (35)$$

where $\alpha_q = \lambda_q/\omega_q$ and yields the transformed Hamiltonian

$$\begin{aligned} \tilde{H} &= \tilde{H}_0 + \tilde{H}_{rc}, \\ \tilde{H}_0 &= (E_e - \epsilon_{eb}) e^\dagger e + \sum_q \omega_q a_q^\dagger a_q, \\ \tilde{H}_{rc} &= g_{rc} \exp \left[- \sum_q \alpha_q (a_q^\dagger - a_{-q}) \right] e + \text{H.c.} \end{aligned} \quad (36)$$

The exciton-boson binding energy $\epsilon_{eb} = \sum_q \lambda_q^2/\omega_q$ that lowers the exciton's energy implicitly indicates its bosonic dressing. However, it is assumed to be modest, i.e. $\epsilon_{eb} \ll E_e$. As before the initial wave function is obtained, neglecting \tilde{H}_{rc} , as the ground state of \tilde{H}_0 in the sector with an exciton $|\psi_0\rangle = e^\dagger|0\rangle$, having energy $E_e - \epsilon_{eb}$.

Switching on \tilde{H}_{rc} the exciton starts to decay and we evaluate the recombination rate Γ using the FGR again, now written in form of an integral

$$\begin{aligned} \Gamma &= -2Im \langle \psi_0 | \tilde{H}_{rc} \frac{1}{\omega + E_0 - \tilde{H}_0} \tilde{H}_{rc} | \psi_0 \rangle \\ &= 2Im i \langle \psi_0 | \tilde{H}_{rc} \int_0^\infty dt e^{i\omega t} e^{-i(\tilde{H}_0 - E_0)t} \tilde{H}_{rc} | \psi_0 \rangle. \end{aligned} \quad (37)$$

where E_0 is the g.s. energy in the sector without exciton. Taking into account well known relations for coherent states (since $\tilde{H}_{rc}|\psi_0\rangle$ is a coherent state)

$$\langle \psi_0 | \tilde{H}_{rc} e^{-i(\tilde{H}_0 - E_0)t} \tilde{H}_{rc} | \psi_0 \rangle = g_{rc}^2 \exp \left[\sum_q \alpha_q^2 (e^{-i\omega_q t} - 1) \right], \quad (38)$$

we finally get

$$\Gamma = 2g_{rc}^2 Re \int_0^\infty dt \exp [i\omega t + \sum_q \alpha_q^2 (e^{-i\omega_q t} - 1)]. \quad (39)$$

Here Γ should be evaluated at $\omega = E_e - \epsilon_{eb}$, which is the difference in the g.s. energy of \tilde{H}_0 in the sector with and without the exciton.

A. Saddle point approximation

While Eq. (39) can easily be evaluated numerically for arbitrary parameters, i.e. the coupling strength g_{rc} and dispersions λ_q, ω_q , it is instructive to get result in a form that reveals the relevant quantities entering Γ . For this purpose we first simplify the general dispersions λ_q, ω_q by assuming that the boson coupling function $g(\omega)$ has mean energy ω_0 and a σ spread around that value, fixing the form

$$g(\omega) = \sum_q \alpha_q^2 \delta(\omega - \omega_q) = \frac{\xi}{\sqrt{2\pi}\sigma} e^{-(\omega - \omega_0)^2/2\sigma^2} \quad (40)$$

with a Gaussian function centered at $\omega = \omega_0$. The dimensionless prefactor $\xi = \sum_q \alpha_q^2$ takes into account the strength of the coupling. Such approximation is well justified for bosons with weak dispersion, e.g. the optical phonons, however it should be reasonable also for the 2D magnons under examination with $\omega_0 \approx J$. Nevertheless, the dispersion $\sigma > 0$ is essential for smooth variation of Γ vs ω , and conceptually crucial for final dispersion of bosons into the system.

The advantage of the form Eq. (40) is that the integral Eq. (39) can be analytically evaluated by saddle point method³⁹, i.e.

$$\int_{-\infty}^{\infty} e^{f(t)} dt \approx e^{f(t_0)} \sqrt{\frac{2\pi}{-f''(t_0)}}, \quad f'(t)|_{t_0} = 0. \quad (41)$$

The function $f(t)$ and its saddle point t_0 , correct up to $\mathcal{O}(\sigma^4/\omega_0^4)$, are in our case

$$f(t) = i\omega t + \xi e^{-i\omega_0 t - \sigma^2 t^2/2},$$

$$t_0 = \frac{i}{\omega_0 + \tilde{\sigma}} \ln\left(\frac{\omega}{\xi(\omega_0 + 2\tilde{\sigma})}\right), \quad (42)$$

where $\tilde{\sigma} = (\sigma^2/2\omega_0) \ln(\omega/\xi\omega_0)$. Then

$$f(t_0) \approx -\frac{\omega}{\omega_0} \left(\ln \frac{\omega}{e\xi\omega_0} - \frac{\sigma^2}{2\omega_0^2} \ln^2 \frac{\omega}{\xi\omega_0} \right) \quad (43)$$

$$f''(t_0) \approx -\omega\omega_0 \left(1 + \frac{\sigma^2}{\omega_0^2} \ln \frac{e\omega}{\xi\omega_0} \right).$$

Since energy transmitted to the bosons equals the MH gap, we insert $\omega = \Delta$. If we neglect also the contributions of order σ^2/ω_0^2 then Γ has especially compact form

$$\Gamma \approx g_{rc}^2 e^{-\xi} \sqrt{\frac{2\pi}{\Delta\omega_0}} \exp\left[-\frac{\Delta}{\omega_0} \ln\left(\frac{\Delta}{e\xi\omega_0}\right)\right]. \quad (44)$$

To test the applicability of Eq. (41) for our case we compare in Fig. 6: a) the numerical evaluation of Γ from Eq. (39), b) the saddle point result for numerically (exactly) established saddle, c) the saddle point result for approximate saddle Eq. (42), and d) compact form of Eq. (44) with $\sigma = 0$.

Let us apply Eq. (44) to the HD exciton recombination due to the emission of spin excitations studied in the previous sections. For that case we set $\omega_0 = J$ and fit Eq. (44) to the

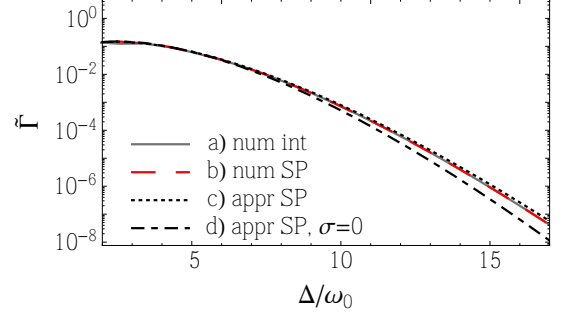


Figure 6. (Color online) Comparison of the result for $\tilde{\Gamma} = \Gamma/g_{rc}^2$, if calculated with a) the numerical evaluation of Γ from Eq. (39), b) the saddle point result for numerically (exactly) established saddle, c) the saddle point result for approximate saddle Eq. (42), and d) compact form of Eq. (44). Parameters $\omega_0 = 5, \xi = 3, \sigma = \omega_0/4$ are used so that numerical integration a) is well defined.

numerically obtained dependence $\Gamma(\Delta)$ for various J , with the dimensionless coupling ξ and prefactor g_{rc} as the fitting parameters. As shown in Fig. 7, formula Eq. (44) captures the dependence $\Gamma(\Delta)$ for ξ that is mildly dependent on J (see Fig. 8). This result has a fundamental importance since it

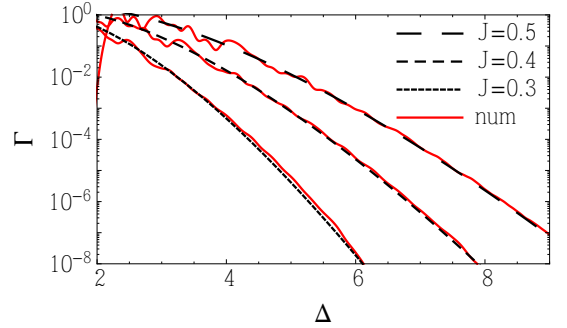


Figure 7. (Color online) Fit of Eq. (44) with ξ, g_{rc} as the fitting parameters to the numerical result (num) for $\Gamma(\Delta)$ obtained on 2D system (as described in previous section) for $J = 0.3, 0.4, 0.5$.

signifies that the recombination of HD bound pair via multi-magnon emission can be described in a much broader frame - as a decay via many bosons. Besides the exponential form the most important message from Fig. 8 is that the effective exciton-boson coupling is very strong $\xi \sim 3$. The dependence of ξ on J resembles ϵ_b/J , where ϵ_b is numerically established binding energy of the HD pair, but with a substantially bigger prefactor. Latter relation is deduced from Eq. (40) if we associate the HD pair binding energy with the exciton-boson binding energy, which might be oversimplified. On the other hand, ξ has milder J dependence yet similar strength as t/J , which would emerge from the n -th order perturbation theory, Eq. (31), taking the charge-spin coupling to be simply the hopping term in Eq. (13). The prefactor dependence $g_{rc} \sim J$ is in qualitative agreement with the original model Eq. (14).

To give a definite comment on which approach, perturbation expansion or exciton-boson model, gives better descrip-

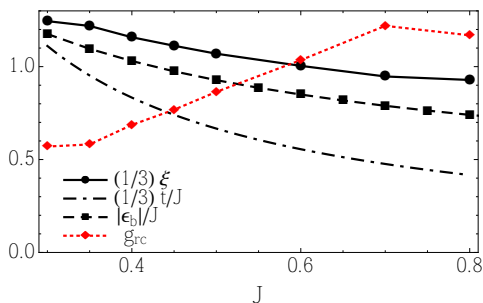


Figure 8. (Color online) Values of the fitting parameters ξ (boson coupling) and g_{rc} (recombination prefactor) as a function of J . For comparison $|\epsilon_b|/J, t/J$ are plotted as well. Prefactor $1/3$ was used with ξ and t/J to unify the scales.

tion could be pointless since they must be essentially intertwined. Still, consideration of exciton coupled to bosons elaborated in this section seems natural and the interpretation of the fitting parameters rather clear: ξ can be identified as the exciton-boson coupling strength, whereas deviation of the value $\alpha_0 \sim 0.8$, Eq. (31), from the expected $\alpha_0 = 2$ could not be argued properly¹⁵. However, probably both, discrepancy in α_0 and lack of quantitative understanding of coupling ξ , originate in the nonperturbative nature of the charge-spin coupling.

VI. COMPARISON WITH EXPERIMENTS AND DISCUSSION

Comparison with experiments: When discussing the application of the theory to cuprates most parameters are well established. The t - J model has been used by many authors for the quantitative comparison of experimental results for various properties. In this sense quite well established parameters are $t \approx 0.35$ eV and $J/t \approx 0.4$, slightly varying within the cuprates. Since the MH gap (or more directly the optical gap) Δ_0 is also determined by optical absorption, the only undetermined parameter is the prefactor t_{rc} , Eq. (14), which we fix to the theoretically obtained $t_{rc} = J/2$. It should be noted that to get Δ relevant for the s-type bound state, as defined in Sec. IV, energy difference to the p-type unbound but optically active state has to be subtracted, $\Delta = \Delta_0 - |\epsilon_b|$. Most pump-probe results are so far obtained for two 2D undoped cuprates: NCO and LCO³. The characteristic microscopic unit time in these systems is given by the elementary process of intercell hopping, i.e. $\tau_0 = \hbar/t \sim 2$ fs.

NCO: Standard values quoted for NCO are³: the optical gap $\Delta_0 = 1.6$ eV and $J = 0.155$ eV, so that $\Delta = 4.1 t$ and from Eq. (29) $\Gamma \sim 2.2 \cdot 10^{-2}/\tau_0$. Finally this leads to $\tau = \Gamma^{-1} \sim 0.09$ ps, which is fairly close to the experimentally measured $\tau \sim 0.2$ ps³.

LCO: Analogous values for LCO are: optical gap $\Delta_0 = 2$ eV and $J = 0.133$ eV, so that $\Delta = 5.3 t$ and $\Gamma \sim 1.3 \cdot 10^{-4}/\tau_0$, yielding $\tau \sim 15$ ps. For this material detailed analysis was not performed, yet it is reported to have considerably longer

relaxation³, consistent with our result. From our theory the difference is quite evident, appearing due to smaller J and larger Δ_0 in the case of LCO.

Effective models: The aim of our theoretical consideration of the problem is to establish the mechanism for the description of the recombination process of photoinduced charged particles in cuprates, based on a minimal sufficient model. Rather than performing the calculations with the prototypical Hubbard model, we canonically transformed it, leading to the model defined by Eqs. (13,14). Its clear advantage is that by separating sectors with different number of HD pairs in lowest order, as suggested by experimentally measured timescales of recombination, a) it assists to extract the excitonic state of bound HD pair from the otherwise complex spectra of Hubbard model, b) takes into account that this state is not an eigenstate (and should therefore decay) in a transparent way - via the creation/recombination term, which serves as a perturbation causing the decay. Since undoped cuprates, being of primer interest of the whole discussion, are actually Mott insulators of the charge-transfer type we derived a similar minimal model also from a more realistic multi-band tight binding model including relevant Cu and O orbitals. Contrary to the previous studies of doped cuprates, hole- and electron-like excitations in this case have to be addressed on equal footing. As observed before the hole-electron (holon-doublon) symmetry is broken in such model²⁹. However, the minimal model describing recombination has similar form with quantitatively comparable strength of operators causing decay of HD pairs as its single-band analogue. Only the internal structure of recombination/creation operators is somewhat richer - allowing new intermediate states. From this we conclude that minimal model derived from the single-band Hubbard is sufficiently good, with a slight modification of Mott gap being interpreted as the charge-transfer gap.

Existence of exciton: Our calculation of the recombination rate relies on the assumption that after being created holon and doublon form a s-type bound state on a timescale shorter than the recombination one. Besides observations in nonlinear optical susceptibility in LCO¹⁷, indirect experimental evidence for formation of such exciton is fluence (pump intensity) independent recombination rate with an exponential decay of charge density. If pairs were not bound, recombination process would depend on the probability to encounter the oppositely charged particle, evidently leading to a non-exponential decay. Since HD pair binds in order to minimize the distortion of short-range ordered spin background in its vicinity, the exciton should cease to exist in experimental conditions when the order is melted, e.g. when pumping the insulator with high fluence or well above the gap.

Validity of Fermi golden rule: Usage of Fermi golden rule seems reasonable since recombination of charged particles is a slow process as compared to the scale \hbar/t of the time-dependent simulations. Still, to test how important are the higher order terms that were neglected we performed the time-dependent evolution of initial excitonic state under Hamiltonian containing the recombination/creation term as well. We observe again an exponential decay of HD pair occupation number. One should beware that such calculation has its lim-

itations too: a) discreteness of spectra sets upper bound for propagation due to recurrence of HD pair, b) virtual processes cause short time oscillations that destabilize the pair yet do not lead to true recombination, c) presence of perturbation alters the whole spectra, shifting the energies and leading to the re-consideration of the definition of the gap, d) we restricted the Hilbert space to the subspace of one and zero HD pairs. Still, the recombination rates obtained with both methods are comparable, and in the larger system with $N = 26$ sites, where finite system artifacts are less pronounced, show slightly faster recombination in time-dependent calculation, as one would expect from the inclusion of additional processes.

Origin of fast recombination: As a result of our study we can conclude that emission of spin excitations can be considered as a plausible mechanism for the non-radiative recombination of photoinduced charges in a MH insulator, in spite of many bosons $n \sim \Delta/J \gg 1$ involved in a simultaneous emission. Feasibility of creation of such large number of spin excitations itself has been demonstrated experimentally by the phonon assisted multimagnon light absorption^{40,41}. The importance of analogous multi-phonon processes has been addressed theoretically as possibly relevant for decay in carbon nanotubes^{33,34}. However, the reason for much faster recombination in MH insulators as compared to the semiconductors⁴ is primarily in strong coupling between charged particles (holons and doublons) and spin background, in addition to obviously larger scale of spin excitations J then the typical phonon energies ω_0 . According to our understanding this strong coupling is manifested in two intertwined observations: a) as revealed by the calculation of spin correlations already the HD exciton involves strong perturbation of the spin AFM background, which can be in the proces of recombination even further enlarged due to possible additional spin flips caused by H_{rc} , b) on the level of effective exciton-boson Hamiltonian the relevant exciton-boson coupling turned out to be strong.

Short-range vs. long-range order: It should be pointed out that the existence of the AFM long-range order and standard magnon excitations is not a necessary precondition for our analysis. The relevant excitations that receive the energy of HD pair are general multiple spin excitations or paramagnons, present also in the paramagnetic phase. All those excitations should have is dispersive nature in order to distribute the local spin perturbation. On the other hand, short-range spin correlations are necessary to provide the dressing of HD pair with spin excitations, and insure the existence of exciton. Other study¹⁴ of decay of unbound uncorrelated holon and doublon in completely spin disordered background revealed very slow recombination, proving the necessity of at least short-range correlated spin-background. After all, our calculations are done in small system which is big enough to accommodate the dressing of HD pair, however does not display long-range order in the strict sense. The role of latter is consequently not present in the result for recombination rate Γ .

Higher photoexcited charge densities: Mechanism for recombination via emission of spin excitations should be relevant for systems with low density of photoexcited carriers that in such conditions presumably form HD excitons. In experiments using high fluence pump pulses, creating high den-

sity of photoexcited charge carriers, other mechanism might become dominant, e.g. so called Auger processes where energy of HD pair is transmitted to other charged carriers created within the pump. When sufficient density of charges is provided, dominance of such processes originates in easier instantaneous energy transmission - simply raising kinetic energy of remaining charge. Clear experimental indication for such processes should be non-exponential decay of particle density, as long as what is observed is not only deviation around the thermal density of charges. The role of reversed, yet similar processes of holon-doublon pair ionization in the initial fast relaxation of doublons excited well above the gap has been established within the DMFT⁴². Moreover, related kinetic-assisted recombination mechanism, possibly consisting of several scattering processes, are dominant in experiments on fermionic cold atoms^{9,10} and in DMFT studies^{11,12}.

Role of dimension: In the present analysis the crucial ingredient for the fast recombination is strong charge-spin coupling. This is inherently present within the 2D (also higher dimensional) strongly correlated system, as modeled within the Hubbard model with $U \gg t$ or the t - J model with $J < t$, where mobile photoexcited or doped charges crucially perturb and frustrate the spin background. On the other and, the physics in 1D correlated system could be quite different due to the phenomenon of charge-spin separation. It is established that e.g. within the 1D t - J model the charge-spin coupling is quite ineffective and the motion of holes/doublons is nearly free for $J \ll t$. Therefore other mechanisms, both for the exciton formation as well as for the HD recombination, have to be invoked to deal with the photoexcited 1D MH insulators.

ACKNOWLEDGMENTS

The authors acknowledge valuable discussions with T. Toyama, R. McKenzie and D. Golež. This work has been supported by the Program P1-0044 and the project J1-4244 of the Slovenian Research Agency (ARRS).

Appendix A: Intra-site Diagonalization for Charge-transfer Hubbard Model

Recombination/creation operator H_{rc} , Eq. (28), derived from the original three-band Hamiltonian, Eq. (15), could have been obtained from higher order perturbative hopping processes, in a similar manner as the exchange coupling in Ref.²⁸. Instead, our derivation of H_{rc} is based on the introduction of states associated with a single cell, where each cell contains a Cu orbital and a Wannier O orbital. Those states represent holon and doublon as well as neutral states and are calculated as the eigenstates of single-cell Hamiltonian H_{0i} , Eq. (16). Coupling between cells is then established by the relevant matrix elements for states on adjacent cells, nontrivial due to hybridization between Cu and O orbitals in the single-cell states. The coupling strengths are set by the Hamiltonian Eq. (17) with Wannier-orbital transformation inherently present in the hopping parameters. As originally proposed

by²⁹, the intra-cell diagonalization that gives us the single-cell states has to be performed within each total spin sector. In the doublet basis, Eq. (19), we diagonalize the Hamiltonian

$$h^{1/2} = \begin{pmatrix} 0 & -\bar{t}_{pd} \\ -\bar{t}_{pd} & \Delta_0 \end{pmatrix} \quad (\text{A1})$$

yielding the g.s. $|g_\sigma\rangle$ that represents the charge-neutral (in the language of single-band Hubbard model spin-like) state with the energy E_g

$$|g_s\rangle = \cos\theta|\bar{d}_s\rangle + \sin\theta|p_s\rangle, \quad (\text{A2})$$

$$E_g = \frac{\Delta_0}{2} \left(1 - \sqrt{1 + \tan^2(2\theta)} \right), \quad (\text{A3})$$

where $\tan 2\theta = 2\bar{t}_{pd}/\Delta_0$.

Within the singlet subspace, Eq. (18), holon is represented by the generalized Zhang-Rice singlet, which in addition to the dominant Zhang-Rice component $(1/\sqrt{2})(\bar{d}_\uparrow^\dagger p_\downarrow^\dagger - \bar{d}_\downarrow^\dagger p_\uparrow^\dagger)|0\rangle$ contains also some fraction of $\bar{d}_\downarrow^\dagger \bar{d}_\uparrow^\dagger|0\rangle, p_\downarrow^\dagger p_\uparrow^\dagger|0\rangle$ states. The fraction of each basis state is obtained by numerical diagonalization of the 3×3 local Hamiltonian. Since $U_d \approx \bar{U}_p + 2\Delta_0$ it turns out satisfactory to use basis

$$\begin{aligned} \{|S_0\rangle &= \frac{1}{\sqrt{2}}(\bar{d}_\uparrow^\dagger p_\downarrow^\dagger - \bar{d}_\downarrow^\dagger p_\uparrow^\dagger)|0\rangle, \\ |S_1\rangle &= \frac{1}{\sqrt{2}}(\bar{d}_\uparrow^\dagger \bar{d}_\downarrow^\dagger + p_\uparrow^\dagger p_\downarrow^\dagger)|0\rangle\}, \end{aligned} \quad (\text{A4})$$

in which local Hamiltonian is

$$h^0 = \begin{pmatrix} \Delta_0 + \bar{V}_{pd} & -2\bar{t}_{pd} \\ -2\bar{t}_{pd} & \frac{1}{2}(U_d + \bar{U}_p) + \Delta_0 \end{pmatrix}, \quad (\text{A5})$$

yielding explicit expression for the holon state $|H\rangle$ and its energy

$$\begin{aligned} |H\rangle &= \cos\phi|S_0\rangle + \sin\phi|S_1\rangle, \quad (\text{A6}) \\ E_H &= \Delta_0 + \bar{V}_{dp} + \frac{U_d + \bar{U}_p - 2\bar{V}_{pd}}{4} \left(1 - \sqrt{1 + \tan^2(2\phi)} \right), \end{aligned}$$

where $\tan 2\phi = 8\bar{t}_{pd}/(U_d + \bar{U}_p - 2\bar{V}_{pd})$. In order to check how much such approximation effects the recombination couplings Eq. (26) for different channels, we compared those values if $|H\rangle$ and E_H are calculated accurately by numerical diagonalization of 3×3 Hamiltonian, or within the latter approximation. The difference in coupling strengths $\delta r = r_{num} - r_{appr}$ is not substantial, as shown in Fig. 9.

The triplet states $|T_s\rangle$ within each cell are decoupled and have energy $E_T = \Delta_0 + \bar{V}_{pd}$.

Appendix B: Effective Hopping Parameters for Charge-transfer Hubbard Model

Hopping parameters that are introduced in the reduced single-band-like Hamiltonian, Eqs. (22,23), are obtained by evaluation of matrix elements for the inter-cell Hamiltonian H_{cc} , Eq. (17), between the states $|H\rangle, |D\rangle, |T_s\rangle, |g_s\rangle$,

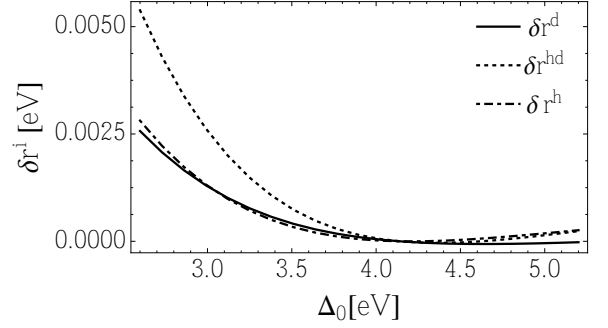


Figure 9. The error in recombination coupling parameters, $\delta r = r_{num} - r_{appr}$, originating in approximate calculation Eq. (A6) of holon state $|H\rangle$ and its energy E_H as a function of Δ_0 . For other parameters standard values are used.

Eqs. (A6,20,A2), on adjacent sites. For example, parameter t^h associated with hopping of holon is calculated from the matrix element $\langle H_i, g_{js} | H_{cc} | g_{is}, H_j \rangle$. Parametrized by θ, ϕ and $\tilde{\tau} = 2t_{pd}\mu_{01}, \tau' = 2t_{pp}\nu_{01}$ they are presented in the Table I.

Holon hopping	$t^h = t_d^h + t_p^h;$ $t_d^h = \tilde{\tau}(\sin 2\theta + \sin 2\phi)/2,$ $t_p^h = \tau' \cos^2(\theta - \phi)/2.$
Doublon hopping	$t^d = t_d^d + t_p^d;$ $t_d^d = \tilde{\tau} \sin 2\theta, \quad t_p^d = \tau' \sin^2 \theta.$
Triplet hopping	$t^{T_0} = t_d^{T_0} + t_p^{T_0}, \quad t^{T_1} = t_d^{T_1} + t_p^{T_1};$ $t_d^{T_0} = \tilde{\tau} \cos 2\theta \sin \phi/2,$ $t_d^{T_1} = \tilde{\tau} \cos 2\theta \sin \phi/\sqrt{2}.$ $t_p^{T_0} = \tau' \cos \theta \cos(\theta - \phi)/2,$ $t_p^{T_1} = \tau' \cos \theta \cos(\theta - \phi)/\sqrt{2}.$
Holon-doublon recombination	$t^r = t_d^r + t_p^r;$ $t_d^r = \tilde{\tau}(\cos \phi + \sin 2\theta \sin \phi)/\sqrt{2},$ $t_p^r = \tau' \cos(\theta - \phi) \sin \theta/\sqrt{2}.$
Triplet-doublon recombination	$t^{r_0} = t_d^{r_0} + t_p^{r_0}, \quad t^{r_1} = t_d^{r_1} + t_p^{r_1};$ $t_d^{r_0} = \tilde{\tau} \cos 2\theta/\sqrt{2},$ $t_d^{r_1} = \tilde{\tau} \cos 2\theta,$ $t_p^{r_0} = \tau' \sin 2\theta/2\sqrt{2},$ $t_p^{r_1} = \tau' \sin 2\theta/2.$

Table I. Hopping parameters for reduced single-band-like Hamiltonian, Eqs. (22,23), parametrized by θ, ϕ and $\tilde{\tau} = 2t_{pd}\mu_{01}, \tau' = 2t_{pp}\nu_{01}$.

These effective hopping parameters are together with the relative energies $\epsilon_H = E_H - E_g, \epsilon_D = -E_g, \epsilon_T = E_T - E_g$ the essential ingredient of recombination coupling strengths, as explicitly written in Eqs. (26).

-
- ¹ K. Matsuda *et al.*, Phys. Rev. B **50**, 4097 (1994).
² H. Okamoto *et al.*, Phys. Rev. B **82**, 060513 (2010).
³ H. Okamoto *et al.*, Phys. Rev. B **83**, 125102 (2011).
⁴ P. Yu and M. Cardon, *Fundamentals of semiconductors: physics and materials properties* (Springer, Berlin, 19996).
⁵ S. Iwai *et al.*, Phys. Rev. Lett. **91**, 057401 (2003).
⁶ H. Uemura, H. Matsuzaki, Y. Takahashi, T. Hasegawa and H. Okamoto, J. Phys. Soc. Jpn. **77**, 113714 (2008).
⁷ T. Miyagoe *et al.*, J. Phys. Soc. Jpn. **77**, 023711 (2008).
⁸ M. Mitrano *et al.*, Phys. Rev. Lett. **112**, 117801 (2014).
⁹ N. Strohmaier *et al.*, Phys. Rev. Lett. **104**, 080401 (2010).
¹⁰ R. Sensarma *et al.*, Phys. Rev. B **82**, 224302 (2010).
¹¹ M. Eckstein and P. Werner, Phys. Rev. B **84**, 035122 (2011).
¹² M. Eckstein and P. Werner, Phys. Rev. Lett. **110**, 126401 (2013).
¹³ H. Aoki *et al.*, Rev. Mod. Phys. **86**, 779 (2014).
¹⁴ R. Sensarma, D. Pekker, A. M. Rey, M. D. Lukin and E. Demler, Phys. Rev. Lett. **107**, 145303 (2011).
¹⁵ Z. Lenarčič and P. Prelovšek, Phys. Rev. Lett. **111**, 016401 (2013).
¹⁶ T. Tohyama, J. Phys. Soc. Jpn. **75**, 034713 (2006).
¹⁷ A. Maeda *et al.*, Phys. Rev. B **70**, 125117 (2004).
¹⁸ D. Salamon *et al.*, Phys. Rev. B **51**, 6617 (1995).
¹⁹ K. A. Chao, J. Spałek and A. M. Oleś, J. Phys. C **10**, L271 (1977).
²⁰ K. A. Chao, J. Spałek and A. M. Oleś, Phys. Rev. B **18**, 3453 (1978).
²¹ A. H. MacDonald, S. M. Girvin and D. Yoshioka, Phys. Rev. B **37**, 9753 (1988).
²² E. Dagotto, Rev. Mod. Phys. **66**, 763 (1994).
²³ S. G. Ovchinnikov and V. Valkov, *Hubbard operators in the theory of strongly correlated electrons* (World Scientific, 2004).
²⁴ V. J. Emery, Phys. Rev. Lett. **58**, 2794 (1987).
²⁵ F. C. Zhang and T. M. Rice, Phys. Rev. B **37**, 3759 (1988).
²⁶ J. Zaanen and A. M. Oleś, Phys. Rev. B **37**, 9423 (1988).
²⁷ A. Ramšak and P. Prelovšek, Phys. Rev. B **40**, 2239 (1989).
²⁸ E. Müller-Hartmann and A. Reischl, Eur. Phys. J. B **28**, 173 (2002).
²⁹ L. F. Feiner, J. H. Jefferson and R. Raimondi, Phys. Rev. B **53**, 8751 (1996).
³⁰ R. Raimondi, J. H. Jefferson and L. F. Feiner, Phys. Rev. B **53**, 8774 (1996).
³¹ T. Tohyama, Phys. Rev. B **70**, 174517 (2004).
³² A. L. Chernyshev, P. W. Leung and R. J. Gooding, Phys. Rev. B **58**, 13594 (1998).
³³ P. Avouris, J. Chen, M. Freitag, V. Perebeinos and J. C. Tsang, Phys. Status Solidi B **243**, 3197 (2006).
³⁴ V. Perebeinos and P. Avouris, Phys. Rev. Lett. **101**, 057401 (2008).
³⁵ A. Avella and F. Mancini, *Strongly Correlated Systems - Numerical Methods* (Springer, Berlin, 2013).
³⁶ T. J. Park and J. C. Light, J. Chem. Phys. **85**, 5870 (1986).
³⁷ R. Englman and J. Jortner, Mol. Phys. **18**, 145 (1970).
³⁸ A. J. Leggett *et al.*, Rev. Mod. Phys. **59**, 1 (1987).
³⁹ P. M. Morse and H. Feshbach, International Series in Pure and Applied Physics, New York: McGraw-Hill, 1953 **1** (1953).
⁴⁰ J. D. Perkins *et al.*, Phys. Rev. Lett. **71**, 1621 (1993).
⁴¹ J. Lorenzana, J. Eroles and S. Sorella, Phys. Rev. Lett. **83**, 5122 (1999).
⁴² P. Werner, K. Held and M. Eckstein, arXiv:1408.3425 (2014).